DOI:
10.1016/j.vascn.2019.106660

Document Version
Publisher's PDF, also known as Version of record

Journal of Pharmacological and Toxicological Methods 102 (2020) 106660

Contents lists available at ScienceDirect

Journal of Pharmacological and Toxicological Methods

journal homepage: www.elsevier.com/locate/jpharmtox

Radiolabelling and immunohistochemistry reveal platelet recruitment into lungs and platelet migration into airspaces following LPS inhalation in mice

S.J. Cleary[a], F. Rauzi[b], E. Smyth[b], A. Correia[a], C. Hobbs[c], M. Emerson[b], C.P. Page[a], S.C. Pitchford[a,*]

[a] Sackler Institute of Pulmonary Pharmacology, Institute of Pharmaceutical Science, King's College London, London, UK
[b] National Heart & Lung Institute, Imperial College London, London, UK
[c] Wolfson Centre for Age-Related Diseases, King's College London, London, UK

ARTICLE INFO

Keywords:
Platelets
Neutrophils
Recruitment
Lungs
LPS

SUMMARY

Introduction: Platelets are under investigation for their role in host defence and inflammatory lung diseases and have been demonstrated to be recruited to the lung. However, the mechanisms and consequences of platelet recruitment into lungs are poorly understood. We have utilised a murine model to investigate the mechanisms of platelet involvement in lung inflammation induced by intranasal administration of LPS.

Objectives: Our aim was to characterise lung platelet recruitment following LPS inhalation in mice using immunohistochemistry, and non-invasive and invasive radiolabelled platelet tracking techniques.

Results: Intranasal administration of LPS caused an increase in lung platelet staining in lung tissue and elicited the recruitment of radiolabelled platelets into the lung. Prior to these responses in the lung, we observed an earlier decrease in blood platelet counts, temporally associated with platelet recruitment to the liver and spleen. Non-invasive measurements of thoracic radioactivity reflected changes in blood counts rather than extravascular lung platelet recruitment. However, both in situ counting of radiolabelled platelets and immunostaining for platelet surface markers showed LPS-induced increases in extravascular platelets into lung airspaces suggesting that some of the platelets recruited to the lung enter air spaces.

Conclusions: Intranasal administration of LPS activates the innate immune response which includes a fall in peripheral blood platelet counts with subsequent platelet recruitment to the lung, spleen and liver, measured by immunohistochemistry and radiolabelling techniques.

1. Introduction

Platelets make important contributions to haemostasis, thrombosis, inflammation and regeneration, and drugs targeting platelets have garnered interest as potential anti-inflammatory interventions for the treatment of inflammatory lung diseases (Amison, Arnold, O'Shaughnessy, et al., 2017; Amison, Momi, Morris, et al., 2015; Li, Zarbock, & Hidalgo, 2017; Middleton, Weyrich, & Zimmerman, 2016; Nachman & Weksler, 1972; Page, 1988; Pitchford, 2006; Semple, Italiano, & Freedman, 2011; Weyrich & Zimmerman, 2013). Observational clinical studies are suggestive of increased survival of patients with chronic obstructive pulmonary disease (COPD) or the acute respiratory distress syndrome (ARDS) receiving anti-platelet treatment (Ekström, Hermansson, & Ström, 2013; Pavasini et al., 2016; Toner, McAuley, & Shyamsundar, 2015). Studies in experimental animals have shown that inflammatory responses depend on platelets in models of allergic airway inflammation (Chae et al., 2016; Pitchford et al., 2003; Pitchford et al., 2004; Pitchford et al., 2005), LPS-induced lung inflammation (Grommes et al., 2012; Kornerup, Salmon, Pitchford, Liu, & Page, 2010), other sterile lung injury models (Looney et al., 2009; Zarbock, Singbartl, & Ley, 2006), and following respiratory infection (Amison, O'Shaughnessy, Arnold, et al., 2018). Furthermore, clinical trials with human volunteers exposed to LPS to assess the potential of anti-platelet drugs to have anti-inflammatory activity, have shown reductions in inflammation following treatment with the anti-platelet drugs clopidogrel, ticagrelor or aspirin (Hamid et al., 2017; Thomas et al., 2015). However, interventional studies carried out so far using existing anti-platelet drugs in more complex clinical settings, for example using aspirin for prevention of ARDS (Kor et al., 2016), and prasugrel to treat allergic asthma (Lussana et al., 2015), have not found clear beneficial effects demonstrating a need for better understanding of how and when to target platelets in the context of inflammatory lung

* Corresponding author.
E-mail address: simon.pitchford@kcl.ac.uk (S.C. Pitchford).

https://doi.org/10.1016/j.vascn.2019.106660
Received 1 July 2019; Received in revised form 21 October 2019; Accepted 1 December 2019
Available online 12 December 2019

diseases.

Many functions of platelets depend on juxtacrine and paracrine signalling which necessitate platelet adhesion on exposed sub-endothelial tissue, endothelium or endothelium-adhesive leukocytes or other platelets (Middleton et al., 2016). Platelet recruitment into lungs has been suggested to be a pathological response occurring in a variety of inflammatory states, including following LPS challenge in guinea pigs (Beijer et al., 1987), rats (Itoh, Cicala, Douglas, & Page, 1996), rabbits (Kiefmann et al., 2004), and mice (Ortiz-Muñoz et al., 2014). Platelets have also been suggested to migrate out of the bloodstream and into tissue and airspaces in inflamed lungs in mouse models of allergic airway inflammation (Pitchford et al., 2008) and following LPS inhalation (Ortiz-Muñoz et al., 2014; Rylander, Beijer, Lantz, Burrell, & Sedivy, 1988), a phenomenon with poorly understood mechanisms and consequences.

Although LPS inhalation has been previously been suggested to cause platelet recruitment to the lungs and lung airspaces of guinea pigs (Beijer et al., 1987; Rylander et al., 1988), lung platelet recruitment following LPS inhalation has not yet been assessed by visualisation of platelets in lung tissues.

We have therefore utilised a mouse model of LPS inhalation similar to those previously suggested to cause platelet-dependent lung neutrophil recruitment (Kornerup et al., 2010), and platelet recruitment and platelet migration into airspaces (Ortiz-Muñoz et al., 2014). The effect of LPS inhalation via intranasal administration on platelet content of lungs was assessed in this model using immunohistochemical staining of CD41 (ITGA2B, α_{IIb}), and using a well-established non-invasive method for tracking radiolabelled platelets (Page, Paul, & Morley, 1982) previously used for measuring pulmonary thromboembolism in mice (Tymvios et al., 2008), as well as radiolabelled platelet biodistribution methods similar to those used in inflammation models (Andonegui et al., 2005; Looney et al., 2009).

2. Methods

2.1. Animals

Female BALB/c mice were purchased from Charles River and used at 6–12 weeks of age. Experiments were approved by King's College London Ethics committee and carried out in accordance with the UK Animals (Scientific Procedures) Act 1986 and EU directive 2010/63/EU. Animal studies are reported in accordance with the ARRIVE guidelines (Kilkenny, Browne, Cuthill, Emerson, & Altman, 2010).

2.2. Intranasal LPS challenge model

Mice were briefly anaesthetised with isoflurane, then challenged via the intranasal route with LPS (O55:B5 from *E. coli*, 5 mg/kg, 2 μl/g), a dose based on previous reports Ortiz-Muñoz et al. (2014) or PBS vehicle, before recovery. This method has previously been shown to deposit ~55% of the delivered dose of LPS in the lungs (Southam, Dolovich, O'Byrne, & Inman, 2002; Su, Looney, Robriquet, Fang, & Matthay, 2004). The terminal anaesthetic used was urethane (3 g/kg i.p. in PBS), given at a time point when neutrophils are detectable in airspaces (+4 h)or at a time point when lung platelet recruitment into lungs has previously been demonstrated (+48 h) (Cleary et al., 2019; Ortiz-Muñoz et al., 2014).

2.3. Buffer solutions

PBS (137 mM NaCl, 3 mM KCl, 8 mM Na_2HPO_4 and 1.5 mM KH_2PO_4, pH 7.3) was made up from tablets (Oxoid). DAB development buffer was made up immediately before use with 1.2 mM DAB (3,3-diaminobenzidine tetrahydrochloride) in 0.1 M Tris buffer (pH 7.6) and 0.03% vol/vol H_2O_2 substrate. Acid-citrate dextrose (ACD) anticoagulant was from Sigma-Aldrich. Calcium and Magnesium-free Tyrode's solution (CFTS) was 134 mM NaCl, 2.7 mM KCl, 5.55 mM D-glucose, 11.9 mM $NaHCO_3$ and 0.21 mM Na_2HPO_4. CFTS was also mixed with ACD (9 volumes of CFTS with 1 volume of ACD) and 2.5 μM of PGE_1 in order to produce Tyrode's-ACD-PGE_1 (TAP) buffer. HEPES-buffered Tyrode's solution contained 20 mM 2-[4-(2-hydroxyethyl)piperazin-1-yl]ethanesulfonic acid (HEPES), 134 mM NaCl, 2.92 mM KCl, 12 mM $NaHCO_3$, 0.34 mM Na_2HPO_4 and 1 mM $MgCl_2$ with the pH adjusted to 7.4.

2.4. Immunohistochemistry

Mice were terminally anaesthetised with urethane, lungs were then collapsed before rapid tracheal cannulation and inflation of lungs with 0.5 ml OCT. The heart was then immediately removed to stop circulation and lungs excised, cut in half laterally, and snap frozen in OCT on a liquid nitrogen-cooled metal heat sink.

Samples were stored at −80 °C, then cryosectioned at 10 μm and air-dried overnight. After fixation (4% vol/vol paraformaldehyde in PBS, 15 min), peroxidase blockade was carried out with 3% vol/vol H_2O_2 in ethanol for 10 min, and blockade of non-specific binding was obtained with 1% w/vol BSA in PBS (also used as a diluent for other reagents) used for 10 min. Samples were then incubated with either biotinylated rat anti-CD41 antibody (MWReg30 clone, Abcam), rabbit anti-CD42b antibody (SP219 clone, Abcam) or a rabbit anti-neutrophil elastase antibody (Polyclonal ab68672, Abcam) (See Supplementary Table 1 for full details of antibody reagents used). After 2 h, slides were washed with PBS, then incubated for 1 h with avidin-biotinylated HRP complex (for staining biotinylated primary, PK-7200, Vector laboratories), or biotinylated anti-rabbit IgG (BA-1000, 1 in 200, Vector laboratories), followed by a further wash and staining with avidin-biotinylated HRP complex for 1 h (for staining unconjugated primary antibodies). Along with the imaging reported in the Figures we stained control samples where primary antibodies were not added to confirm that any staining included in the quantification was not a result of non-specific or off-target binding of reporter antibodies or probes. Thresholds were set on these images during analysis so that any non-target signal would be excluded. Examples of specificity controls have been added to the data supplement (Supplementary Fig. 1). Slides were washed with PBS again, developed with DAB, counterstained with haematoxylin, mounted and coverslipped.

CD41 and neutrophil elastase were also visualised simultaneously by staining with rat anti-CD41 antibody (MWReg30 clone, Abcam) and rabbit anti-neutrophil elastase antibodies (polyclonal ab68672, Abcam), washing with PBS, then incubation with low cross-reactivity AlexaFluor594-conjugated anti-rat IgG and AlexaFluor488-conjugated anti-rabbit IgG (1in500, both Thermo Fisher Scientific), with nuclei counterstained with Hoechst 33258 (Sigma Aldrich).

2.5. Image capture and analysis

Bright field images (six 447 × 596 μm fields from every section) were captured using a 20× objective on a Leica DM 2000 upright microscope.

Using ImageJ with the colour deconvolution vectors plugin (from G. Landini, University of Birmingham, UK), DAB and haematoxylin stains were deconvoluted from RGB images as described elsewhere (Ruifrok & Johnston, 2001). Positivity thresholds were set on DAB signal, and platelets (CD41+, > 1.45μm^2) were counted or neutrophil elastase coverage was quantified using the ImageJ particle analyzer.

Separate blinded analyses were also conducted on the same microscope using a 63× objective to capture 50 image fields of 189 × 142 μm from the respiratory portion of the lung from each mouse in order to enable the visualisation of platelets which appeared outside of blood in the bronchoalveolar space. These extravascular platelets were spatially dis-associated from blood vessels and were manually counted by an independent observer.

Whole lung sections double stained for neutrophil elastase and CD41 using immunofluorescence were also imaged using the InCell Analyzer 6000 with hardware and software autofocus for tiled acquisition. Images were then thresholded, colour channels combined, and tiles stitched as described elsewhere (Preibisch, Saalfeld, & Tomancak, 2009), to quantify bronchial lumen platelets (CD41+, inside lumen of intact epithelium of bronchiole). CD41+ objects with proplatelet-like morphology were identified by size and morphology (area $> 55\ \mu m^2$ and circularity < 0.5) and CD41+ cells (nuclei surrounded by CD41 positivity, megakaryocytes and precursors) were also counted.

2.6. Blood microsampling

Conscious mice were warmed to 37 °C for 10 min in a surgical recovery chamber. A 1–2 mm cut was made across a lateral tail vein and blood was collected using a micropipette tip, and dispensed into stromatol for counting platelets, Turk's solution for counting leukocytes, and used to make a smear for leukocyte differential counts with Kwik-Diff stain.

2.7. Platelet radiolabelling

Blood for isolation of platelets was collected by cardiac puncture from donor mice under anaesthesia into 100 µl ACD, and platelet rich plasma was separated by centrifugation (3 min at 300 rcf, PRP removed, 400 µl TAP buffer added, 3 min at 300 rcf, further PRP removed, with red cells sedimented out with 2 min at 200 rcf). Platelets were then separated from plasma (7 min at 1500 rcf), and resuspended in 600 µl TAP buffer per 4 donor mice at a mean concentration of $6 \pm 1 \times 10^8$ platelets/ml. The platelet suspension was then added to a 5:1 mixture of 1.8 MBq of $^{111}InCl_3$ in sterile 0.9% w/vol saline (Mallinckrodt) and 90 mM tropolone in HEPES-buffered Tyrode's solution, and allowed to label for 10 min at room temperature. The platelet suspension was centrifuged again and resuspended in 960 ml CFTS for immediate intravenous infusion of 200 µl per mouse (mean labelling efficiency: 62 ± 5%, $2.5 \pm 0.5 \times 10^8$ labelled platelets per mouse). Platelets were allowed to equilibrate in the mouse for at least 1 h before beginning measurements.

2.8. Non-invasive recordings of thoracic platelet content

We utilised a previously described non-invasive method for measuring continuous platelet recruitment into the thoracic region (Page et al., 1982) that has been used for measuring lung platelet recruitment into the lungs of guinea-pigs following LPS inhalation (Beijer et al., 1987) or following intravenous LPS infusion in rats (Itoh et al., 1996). This method has more recently been adapted for use in mice (Tymvios et al., 2008). Thus, a SPEAR probe, calibrated to detect photon energies from decay of Indium-111, was placed over the thorax and collimated with 6 mm lead sheeting to maximise detection of platelet associated radioactivity in the thorax and used to measure increases in platelet recruitment in the pulmonary circulation following intravenous administration of 4 mg/kg ADP, relative to background signal from resting platelet associated radioactivity in the pulmonary circulation. The presence of viable, circulating radiolabelled platelets 48 h after transfusions was also confirmed by positive responses to i.v. administration of ADP and measurements of platelet vs. plasma associated radiolabel content. Repeated measurements in the same mouse over hours and days were made possible using a cradle which positioned the thorax of the mouse in a fixed position under the lead collimated SPEAR gamma detector relative to a tooth bar on the isoflurane mask used to maintain general anaesthesia. Means of thoracic radioactivity over 5 min periods were taken and the data were normalised to baseline (pre-intranasal dosing with PBS or LPS).

2.9. Biodistribution of radiolabelled platelets in organs, blood and BAL

Mice transfused with radiolabelled platelets were terminally anaesthetised with urethane and whole blood collected by cardiac puncture with 100 µl rapidly decanted for gamma counting. BAL fluid (3× washes of 0.5 ml PBS), and lung, liver and spleens were also collected.

The percentage of the injected dose of radioactivity in whole blood (100 µl), lungs, liver, spleen and BAL (800 µl, divided into cell pellet and supernatant by centrifugation at 1500 rcf for 7 min) was measured by gamma counting of samples and 1% injected dose controls using a Wallac Compugamma 1282 system. Using a similar method to those employed by others (Andonegui et al., 2005; Looney et al., 2009), platelet recruitment from blood to organs was quantified by dividing the quantity of radiolabel detected in whole, non-perfused organs by the quantity of signal remaining in blood.

Inflammatory responses were confirmed by counting BAL leukocytes using total cell counts and differential counts of Kwik-Diff stained cytospin preparations.

2.10. Statistics

Data are presented as means ± standard error and graphed and analysed using GraphPad Prism 7.0. Group comparisons were made using unpaired or paired *t*-tests, or 2-way ANOVA or ANCOVA with single or repeated measures, and baseline values fit as covariates where appropriate, followed by Holm's test for within-time point effects following LPS inhalation. Data were log transformed as required and $P < .05$ was used as the threshold for statistical significance.

3. Results

3.1. LPS inhalation via intranasal administration results in increased platelet recruitment to lungs

Mice were administered LPS or PBS intranasally, and blood and lungs were collected 4 h and 48 h afterwards for immunohistochemical analysis of platelets (Fig. 1A & B). In separate experiments, mice subjected to this protocol were transfused with ^{111}In-labelled platelets detected non-invasively using a gamma radiation probe. 48 h after LPS exposure, a time point when lung platelet recruitment was reported to occur in a previous study (Ortiz-Muñoz et al., 2014), increases in both lung platelet staining (Fig. 1C), and lung radiolabelled platelet recruitment were detected (Fig. 1E).

3.2. LPS inhalation via intranasal administration causes an initial temporary thrombocytopenia

Intranasal LPS administration initially elicited a fall in platelet counts in the peripheral circulation, as measured by serial blood microsampling (Fig. 1D), and the quantity of radiolabelled platelets remaining in blood at 4 h after intranasal challenge (Fig. 1E). By 48 h following intranasal challenge, there was no significant difference in blood platelet counts (Fig. 1D) or in the retention of radiolabelled platelets in blood between LPS treated mice and PBS controls (Fig. 1F), providing evidence that increases in lung platelet staining were not because of increased circulating platelet counts, and increases in the lung:blood ratio were unlikely due to decreases in blood platelet retention.

3.3. LPS inhalation via intranasal administration causes a temporary decrease in radiolabelled platelet content in the thoracic region

Given that histological methods require cohorts of mice to be sacrificed at various time points to allow microscopical analysis of tissue slices, and accumulation of radiolabelled platelets in organs via gamma counting requires terminal removal of blood and organs, we attempted

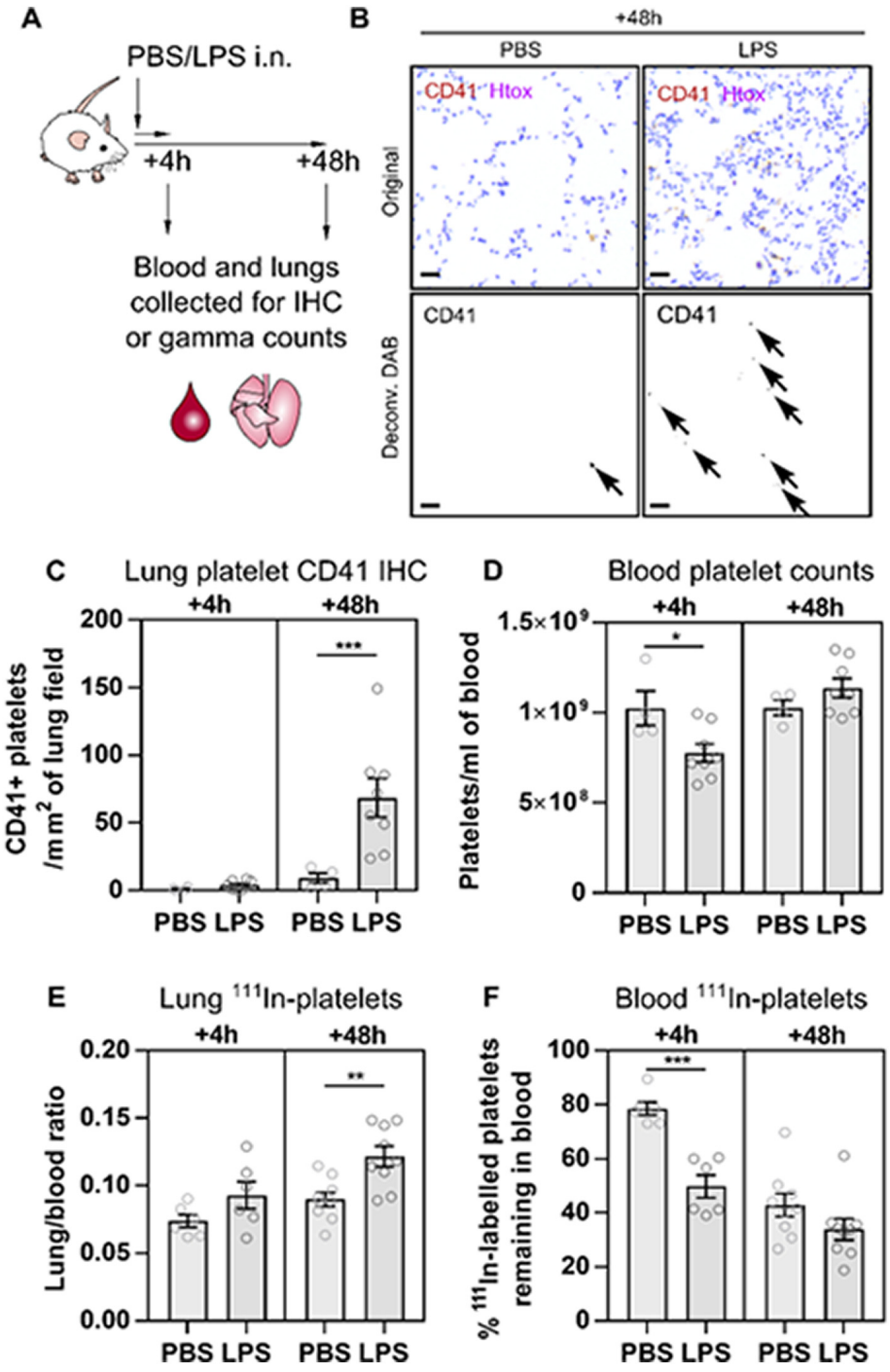

Fig. 1. LPS inhalation causes platelet recruitment to the lungs. (A) Mice were administered PBS or LPS intransally, and lungs harvested at 4 h and 48 h for immunohistochemical analysis and enumeration of gamma-radiation counts. In some experiments, mice were administered ^{111}In-labelled platelets intravenously 1 h before LPS. (B) Platelets were enumerated with ImageJ using colour deconvolution and particle analysis. Original RGB colour images with CD41 staining in brown and haematoxylin staining in blue were deconvoluted to split the colour channels corresponding to DAB staining in a separate greyscale image. An intensity threshold was then set on the greyscale image to define areas of positivity. Particle analysis was then used to count platelet sized objects in the lungs (C), and separately, platelet enumeration was in peripheral blood of same groups of mice (D). ^{111}In-labelled platelet radioactivity of the lungs (E). % of injected ^{111}In-labelled platelet radioactivity remaining in the blood (F). Data is mean ± standard error. Immunohistochemistry conducted on PBS groups $n = 4$, LPS groups $n = 8$. Radiolabelled platelet data conducted with $n = 6$ (4 h), $n = 9$ (48 h), 2-way ANOVA with Holm's test for LPS effect within time points, * = $P < .05$, ** = $P < .01$, *** = $P < .001$ as indicated. Scale bar = 20 μm. (For interpretation of the references to colour in this figure legend, the reader is referred to the web version of this article.)

to use a non-invasive technique, previously used to measure thromboembolic responses in mice (Tymvios et al., 2008), to measure intrathoracic platelet accumulation in individual mice and therefore reduce animal use. This technique required the placement of a gamma probe above the thoracic cavity of anaesthetised mice to record ^{111}In-labelled platelet accumulation via a spectrometer recording onto a computer (Fig. 2A). Thus, an increase in platelet accumulation in the thorax can be observed after the intravenous administration of ADP (Fig. 2B & 2C). Conversely, the intravenous administration of LPS revealed no immediate impact on platelet accumulation into the thoracic region of terminally anaesthetised mice (Fig. 2D). Furthermore, mice administered intranasal LPS had decreased thoracic radioactivity compared to PBS controls at 4 h after challenge, correlating with the decrease in blood platelet signal at 4 h after LPS inhalation (Cleary et al., 2019), but no effect of LPS inhalation on thoracic radiolabelled platelet content was measured at 24 or 48 h after LPS inhalation (Fig. 2E). Normalising data from LPS-treated mice to that from PBS vehicle controls to account for anticipated normal platelet lifespan in the circulation, and then to correct for the estimated actual content of radiolabelled platelets in blood measured at +4 and + 48 h from intranasal challenge, suggested that the LPS-induced decrease in thoracic signal was smaller than the effect of LPS on reducing blood platelet counts (Supplementary Fig. 2A-C). This difference is suggestive that non-invasive measurements of the lung platelet recruitment response may be possible with the use of more sophisticated methods incorporating measurements of blood radiolabelled platelet content, blood volume and 3D scanning to enable focus on the pulmonary vasculature.

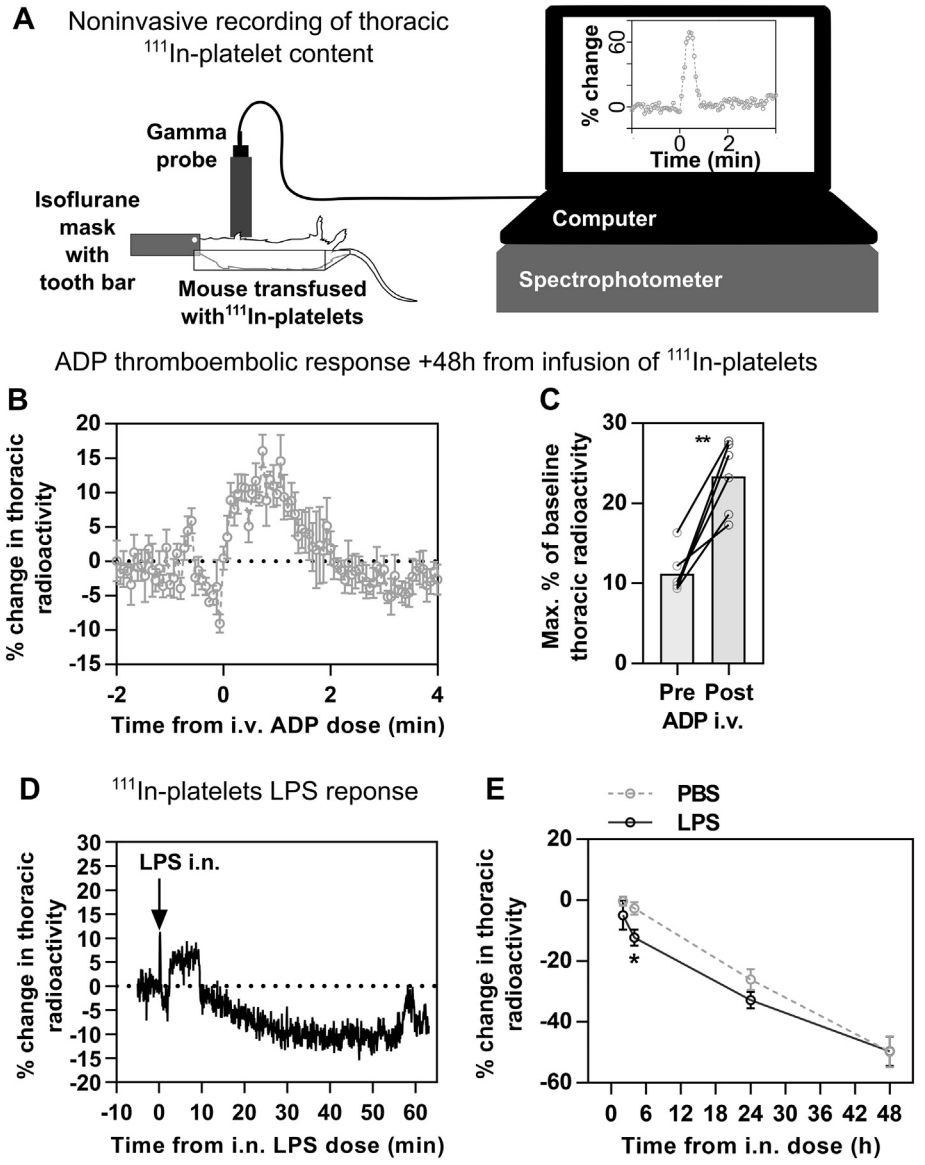

Fig. 2. Use of Gamma-radiation probe to detect lung platelet accumulation. Mice transfused with ^{111}In-labelled platelets were anaesthetised using isoflurane, with repeated recordings made over the same region of thorax by clamping a gamma detector at a fixed position relative to a tooth bar and custom cradle attached to the isoflurane mask. Signal from the gamma detector was de-convoluted using a UCS30 spectrophotometer and data logged on a computer running USX software (A). Responses to i.v. injections of 4 mg/kg ADP in mice infused 48 h previously with ^{111}In-labelled platelets (B). Analysis of pre and post ADP signal showing maximal percentage increases in time periods relative to the baseline (C). Single trace showing acute response to intranasal LPS (5 mg/kg) inhalation in a terminally anaesthetised mouse (D). Measurements of thoracic radioactivity were made at 0, 2, 4, 24, and 48 h after intranasal challenge with LPS, data shown as % change from time 0 h (E). Data are mean ± standard error where error bars are shown. ADP data: n = 6, comparison is paired *t*-test. LPS data *n* = 5, two way ANCOVA with baseline values fit as covariates, with repeated measures and Holm's test for effects of LPS inhalation within time points. * = P < .05, ** = *P* < .01.

3.4. LPS inhalation via intranasal administration increases the content of radiolabelled platelets in liver and spleen

The liver and the spleen are major sites of platelet clearance from the circulation (Kaplan & Saba, 1978). We therefore investigated whether the peripheral thrombocytopaenia recorded 4 h after LPS exposure was due to the accumulation of platelets into these organs and we observed increases in liver and spleen platelet recruitment associated with the initial thrombocytopenia at this time point (Fig. 3A & 3B).

3.5. LPS inhalation via intranasal administration causes diapedesis of platelets into lung airspaces

The quantity of radiolabelled platelets was measured in BAL fluid cell pellets and supernatant. No effect of LPS was detected 4 h after LPS inhalation, but by 48 h after intranasal challenge with LPS, the BAL radiolabel content in mice was increased (Fig. 4A). A readout of 0.01% of injected dose corresponds to approximately 27,500 platelets per ml of BAL fluid.

Sections of lung from mice exposed to LPS or PBS controls were also stained for immunofluorescent labelling of CD41 (Fig. 4B) in order to visualise platelets in airspaces and overcome the problem of false positive staining found around respiratory epithelium when using DAB reporters. A survey of small intact airways revealed CD41+ platelets associated with cells, some of which were neutrophil elastase positive, and others were not (Fig. 4B). Quantitative analysis revealed a small, yet significant accumulation of platelets in the bronchial lumen 48 h after LPS administration (Fig. 4C). However, it should be noted that LPS administration induces significant inflammation around small blood vessels and alveolar-capillary units more distal in the lung parenchyma. Therefore, images of fields of alveolar-capillary networks also stained for platelets. These sections were stained for the platelet antigen CD42b, which was found to provide a stronger staining signal than the CD41 method (Cleary et al., 2019). Sections were captured with a high-power 63× objective and used for manual counting of platelets that were not visibly within alveolar capillaries or pulmonary blood vessels and so appeared extravascular in the alveolar airspaces (Fig. 4D). LPS inhalation caused a significant increase in the number of extravascular platelets (PBS vs. LPS: 55 ± 5 plts per mm^2 vs. 252 ± 65 plts per mm^2. Fig. 4E).

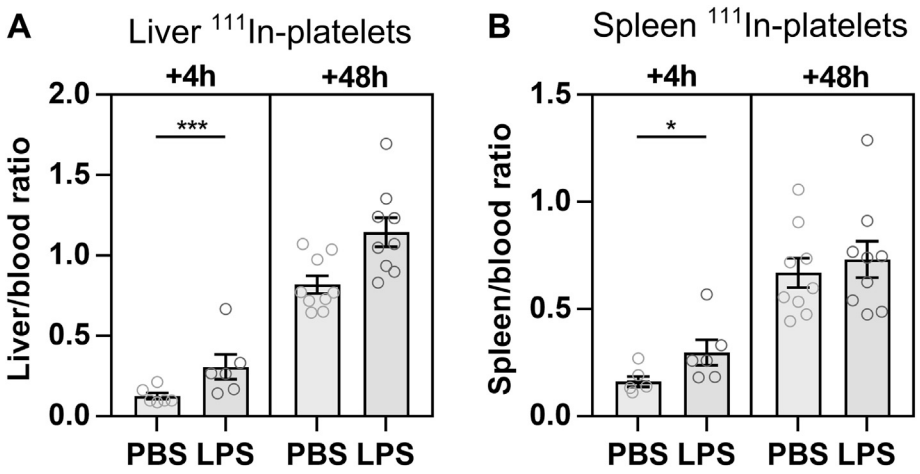

Fig. 3. LPS inhalation causes increases in liver and spleen platelet recruitment. Mice were administered ^{111}In-labelled platelets intravenously, then PBS or LPS intranasally. Livers, spleens, and blood were collected at 4 and 48 h after intranasal challenge. The % ^{111}In-labelled platelet radioactivity of the liver or spleen was divided by the % of injected ^{111}In-labelled platelet radioactivity remaining in the blood to measure (A) liver platelet recruitment, (B) spleen platelet recruitment. Mean ± standard error, 4 h time point: n = 6, 48 h time point: n = 9, 2-way ANOVA with Holm's test for LPS effect within time points, * = P < .05, *** = *P* < .001.

3.6. LPS inhalation via intranasal administration increases the quantity of CD41+ events with proplatelet or megakaryocyte-like morphology in the lungs

Recent estimates suggest that around half of blood platelets originate from megakaryocyte fragmentation in the pulmonary circulation in healthy mice (Lefrançais et al., 2017). However, previously reported methods did not allow for discrimination of megakaryocytes from proplatelets or platelet aggregates in inflamed lungs (Ortiz-Muñoz et al., 2014). Immunofluorescence and tiled acquisition and stitching allowed for improved identification of CD41+ events with proplatelet morphology (Fig. 5A) and CD41+ cells with large nuclei consistent with the appearance of megakaryocytes (Fig. 5B), with both populations increased in number in lungs following LPS inhalation (Fig. 5C, D).

4. Discussion

We present here evidence that LPS can induce platelet recruitment into the lungs and airspaces which we have detected with immunohistochemistry and by monitoring the recruitment of radiolabelled platelets following an initial decrease in platelet counts in the peripheral circulation.

Our initial aim was to measure increases in the quantity of lung platelets by detecting an increase in thoracic radioactivity as previously achieved in guinea pigs following exposure to aerosolised LPS (Beijer et al., 1987). Measurement of lung platelet recruitment using this method was likely confounded by a decrease in blood platelets more closely temporally associated with increases in liver and spleen platelet content rather than with lung platelet recruitment, and possibly also by changes in the blood content of either the lung or of the systemic vasculature beneath the detector probe. As this relatively simple platelet monitoring method was not successful in measuring lung platelet recruitment, we would recommend that future approaches employ blood microsampling (to monitor changes in the radiolabelled platelet content of blood over time), 3-dimensional single-photon emission computed tomography imaging methods (to permit exclusive focus on the pulmonary vasculature), and co-administration of differentially labelled red blood cells to control for regional alterations in blood supply (Doerschuk et al., 1990). However, previously in this model we have measured flux of non-adhesive platelets in LPS-challenged lung microvasculature and in PBS controls, and found no difference, suggestive of a lack of LPS-induced alteration in pulmonary blood flow (Cleary et al., 2019). These approaches may enable repeated non-invasive measurements of lung radiolabelled platelet recruitment in mice and combined with fate-tracking imaging methods might provide answers to the question of whether platelets recruited to the lung come from the blood pool or are released secondary to their retention in spleen or liver. The development of real-time imaging techniques to measure platelet recruitment would allow these advances to be made with the use of fewer animals and without use of procedures in conscious animals, in line with European and UK legislation requiring animal procedures to be conducted with consideration to reduction, refinement and replacement.

The successful quantification of immunostained lung platelets and blood platelets using microsampling shows ready promise for use of these methods in investigation of the molecular and cellular basis of platelet responses in response to inflammatory and pathogenic stimuli (Cleary et al., 2019).

Detection of increased platelet content in BAL fluid, within the lumen of bronchioles, and in extravascular alveolar spaces are consistent with previous reports of LPS-induced diapedesis of platelets into lung tissue (Ortiz-Muñoz et al., 2014), and following bacterial infection of the lung (Amison et al., 2018). Visualisation of platelet diapedesis using intravital microscopy, and platelet-specific knockout of adhesion molecules are required to provide further evidence for these phenomena reflecting directed platelet migration across the endothelial and epithelial barriers, as previously shown in lungs of allergic mice following allergen challenge (Pitchford et al., 2008).

Increases in lung content of CD41+ nucleate cells and anucleate proplatelets following LPS inhalation are suggestive of effects of LPS on lung thrombopoiesis, although dynamic lung imaging and measurements of megakaryocytes and proplatelets in blood and bone marrow are required to determine to what extent these images are due to alterations in lung-derived megakaryocyte precursors or bone marrow release, pulmonary trapping or retention of megakaryoctyes and proplatelets (Lefrançais et al., 2017).

In summary, we have found that exposure of mice to inhaled LPS caused temporally distinct increased lung, liver and spleen platelet recruitment while decreasing blood platelet content, and hope that the methods described in the present study for measuring these responses will help with future experimentation designed to increase our understanding of the involvement of platelets in lung inflammation and host defence.

Authorship

S.J.C. designed and performed the research, analysed the data, and wrote the paper. C.H. contributed to assay development. F.R., E.S., A.C., C.H., performed research. C.P.P. designed research and helped write paper. M.E., and S.C.P. proposed the project, designed research and wrote paper.

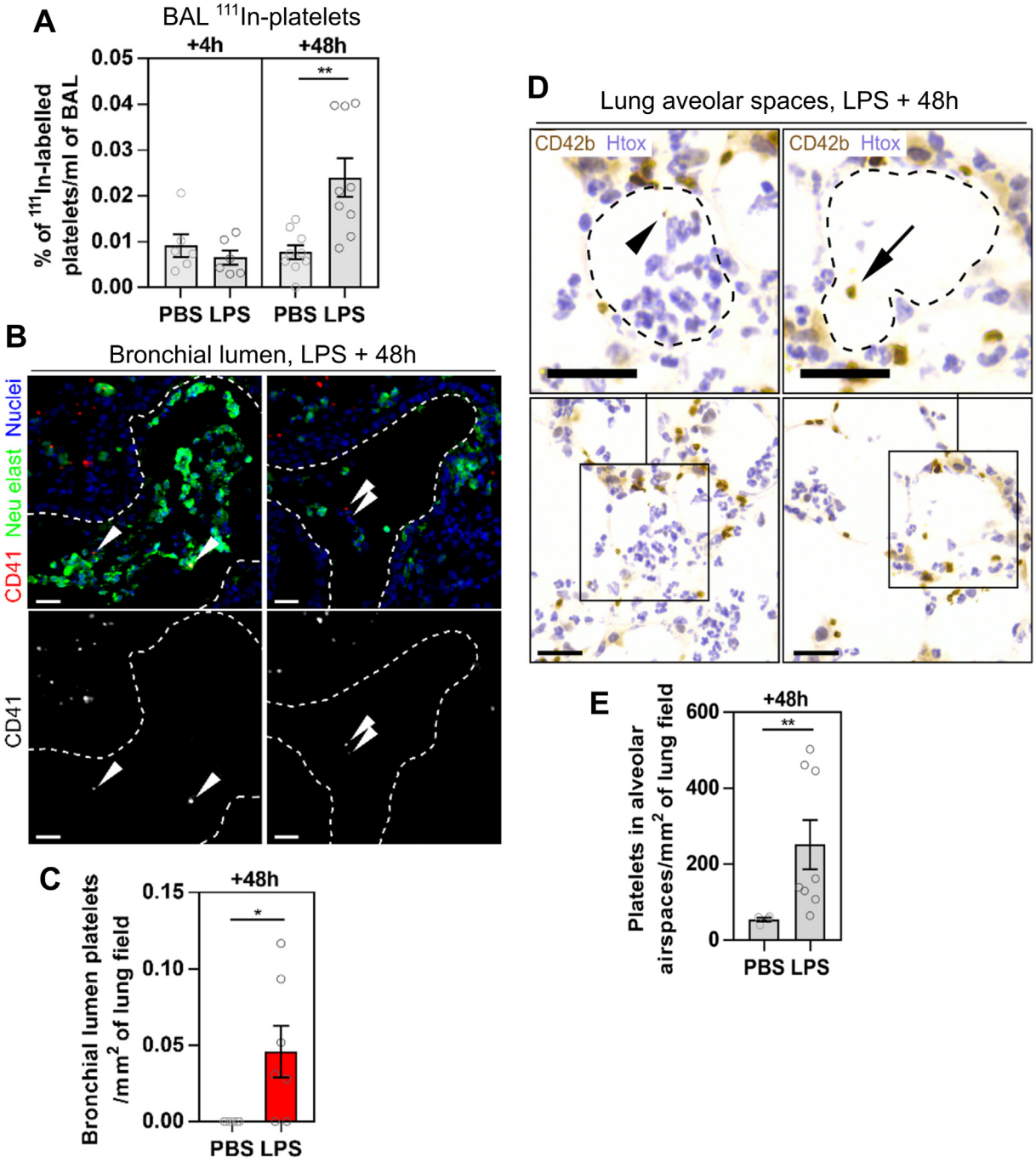

Fig. 4. Evidence for platelet migration into airspaces following LPS inhalation. Mice were administered PBS or LPS intranasally, and lungs harvested at 48 h for immunohistochemical analysis. In some experiments, mice were administered ^{111}In-labelled platelets intravenously 1 h before LPS and BAL fluid was collected at 4 and 48 h after LPS exposure and ^{111}In-platelet content quantified. (A) ^{111}In-platelet content in BAL fluid. (B) Airways (dashed line) were identified in lung sections stained for CD41 (red), neutrophil elastase (green) and nuclei (blue) (top panels). Bottom panels: CD41 stain only. Airway lumen platelets are highlighted with arrowheads. Scale bar: 20 μm. (C) The number of CD41+ platelets within airways was quantified and expressed as number per total area of sections surveyed. (D) Lung sections immunostained for CD42b (brown) with haematoxylin counterstain (blue). Platelets appearing extravascularly with intra-alveolar neutrophils (black arrowhead) and alone (black arrow) inside alveolar airspaces (dotted lines) are shown.(E) Quantification of CD42b + platelets detected in alveolar airspaces. Data are mean ± standard error. Radiolabelled platelet data conducted with n = 6 (4 h), n = 9 (48 h), 2-way ANOVA with Holm's test for LPS effect within time points. Immunohistochemistry data with conducted with PBS: n = 6 and LPS: *n* = 7 (CD41 data), or PBS: n = 4, LPS: n = 8 (CD42b data). Comparisons are Mann-Whitney test. * = P < .05, ** = P < .01. Scale bars = 20 μm. (For interpretation of the references to colour in this figure legend, the reader is referred to the web version of this article.)

Funding Acknowledgement

This research was funded by a Medical Research Council Doctoral Training Grant (MRC-DTP), associated in vivo strategic skills funds awarded to Dr. Simon Pitchford to fund Simon Cleary; and by a NC3Rs research grant (NC/M000079/1) awarded to Dr. Simon Pitchford and Dr. Mike Emerson.

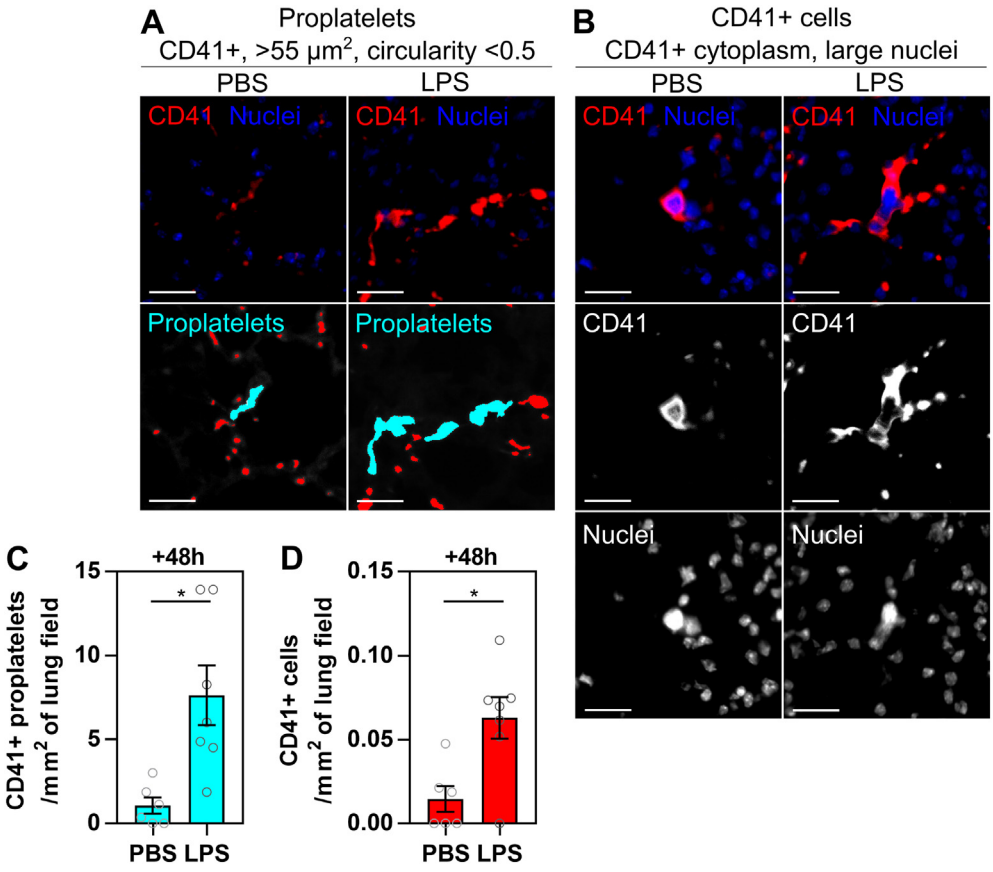

Fig. 5. Evidence for increased lung megakaryocyte and proplatelet content following LPS inhalation. Mice were given intranasal PBS vehicle or LPS (5 mg/kg) and lungs collected 48 h later. (A) Using tiled scans of whole left lung sections, ImageJ was used to identify objects with proplatelet morphology by their CD41 positivity, increased size (> 55 μm^2), and lower circularity (< 0.5 4π(area/perimeter^2)) relative to platelets, and (B) CD41+ cells were manually counted in a blinded fashion by scanning across sections to count large nuclei surrounded by CD41+ cytoplasm. (C) Quantification of proplatelet and (D) CD41+ cell frequencies. PBS: n = 6, LPS $n = 7$. Comparisons are unpaired t-test or Mann-Whitney U test, * = $P < .05$. Scale bars = 50 μm.

Declaration of Competing Interest

The authors declare that they have no known competing financial interests or personal relationships that could have appeared to influence the work reported in this paper.

Appendix A. Supplementary data

Supplementary data to this article can be found online at https://doi.org/10.1016/j.vascn.2019.106660.

References

Amison, R. T., Arnold, S., O'Shaughnessy, B. G., et al. (2017). Lipopolysaccharide (LPS) induced pulmonary neutrophil recruitment and platelet activation is mediated via the P2Y1 and P2Y14 receptors in mice. *Pulmonary Pharmacology & Therapeutics, 45*, 62–68.

Amison, R. T., Momi, S., Morris, A., et al. (2015). RhoA signaling through platelet $P2Y_1$ receptor controls leukocyte recruitment in allergic mice. *The Journal of Allergy and Clinical Immunology, 135*, 528–538.

Amison, R. T., O'Shaughnessy, B. G., Arnold, S., et al. (2018). Platelet depletion impairs host defence to pulmonary infection with *Pseudomonas aeruginosa* in mice. *American Journal of Respiratory Cell and Molecular Biology, 58*, 331–340.

Andonegui, G., Kerfoot, S. M., McNagny, K., Ebbert, K. V. J., Patel, K. D., & Kubes, P. (2005). Platelets express functional toll-like receptor-4. *Blood. 106*, 2417–2423.

Beijer, L., Botting, J., Crook, P., Oyekan, A. O., Page, C. P., & Rylander, R. (1987). The involvement of platelet activating factor in endotoxin-induced pulmonary platelet recruitment in the guinea-pig. *British Journal of Pharmacology, 92*, 803–808.

Chae, W.-J., Ehrlich, A. K., Chan, P. Y., Teixeira, A. M., Henegariu, O., Hao, L., et al. (2016). The Wnt antagonist Dickkopf-1 promotes pathological type 2 cell-mediated inflammation. *Immunity. 44*, 246–258.

Cleary, S. J., Hobbs, C., Amison, R. T., Arnold, S., O'Shaughnessy, B. G., Lefrançais, E., ... Pitchford, S. C. (2019). LPS-induced lung platelet recruitment occurs independently from neutrophils, PSGL-1, and P-selectin. *American Journal of Respiratory Cell and Molecular Biology*. https://doi.org/10.1165/rcmb.2018-0182OC.

Doerschuk, C. M., Downey, G. P., Doherty, D. E., English, D., Gie, R. P., Ohgami, M., ... Hogg, J. C. (1990). Leukocyte and platelet margination within microvasculature of rabbit lungs. *Journal of Applied Physiology (Bethesda, MD: 1985), 68*, 1956–1961.

Ekström, M. P., Hermansson, A. B., & Ström, K. E. (2013). Effects of cardiovascular drugs on mortality in severe chronic obstructive pulmonary disease. *American Journal of Respiratory and Critical Care Medicine, 187*, 715–720.

Grommes, J., Alard, J. E., Drechsler, M., Wantha, S., Mörgelin, M., Kuebler, W. M., et al. (2012). Disruption of platelet-derived chemokine heteromers prevents neutrophil extravasation in acute lung injury. *American Journal of Respiratory and Critical Care Medicine, 185*, 628–636.

Hamid, U., Krasnodembskaya, A., Fitzgerald, M., Shyamsundar, M., Kissenpfennig, A., Scott, C., et al. (2017). Aspirin reduces lipopolysaccharide-induced pulmonary inflammation in human models of ARDS. *Thorax. 72*, 971–980.

Itoh, H., Cicala, C., Douglas, G. J., & Page, C. P. (1996). Platelet accumulation induced by bacterial endotoxin in rats. *Thrombosis Research, 83*, 405–419.

Kaplan, J. E., & Saba, T. M. (1978). Platelet removal from the circulation by the liver and spleen. *The American Journal of Physiology, 235*, H314–H320.

Kiefmann, R., Heckel, K., Schenkat, S., Dörger, M., Wesierska-Gadek, J., & Goetz, A. E. (2004). Platelet-endothelial cell interaction in pulmonary micro-circulation: The role of PARS. *Thrombosis and Haemostasis, 91*, 761.

Kilkenny, C., Browne, W. J., Cuthill, I. C., Emerson, M., & Altman, D. G. (2010). Improving bioscience research reporting: The ARRIVE guidelines for reporting animal research. *PLoS Biology, 8*, e1000412.

Kor, D. J., Carter, R. E., Park, P. K., Festic, E., Banner-Goodspeed, V. M., Hinds, R., et al. (2016). Effect of aspirin on development of ARDS in at-risk patients presenting to the emergency department. *JAMA, 315*, 2406.

Kornerup, K. N., Salmon, G. P., Pitchford, S. C., Liu, W. L., & Page, C. P. (2010). Circulating platelet-neutrophil complexes are important for subsequent neutrophil activation and migration. *Journal of Applied Physiology, 109*, 758–767.

Lefrançais, E., Ortiz-Muñoz, G., Caudrillier, A., Mallavia, B., Liu, F., Sayah, D. M., et al. (2017). The lung is a site of platelet biogenesis and a reservoir for haematopoietic progenitors. *Nature. 544*, 105–109.

Li, J. L., Zarbock, A., & Hidalgo, A. (2017). Platelets as autonomous drones for hemostatic and immune surveillance. *The Journal of Experimental Medicine*. https://doi.org/10.1084/jem.20170879 pii: jem.20170879.

Looney, M. R., Nguyen, J. X., Hu, Y., Van Ziffle, J. A., Lowell, C. A., & Matthay, M. A. (2009). Platelet depletion and aspirin treatment protect mice in a two-event model of transfusion-related acute lung injury. *The Journal of Clinical Investigation, 119*, 3450.

Lussana, F., Di Marco, F., Terraneo, S., Parati, M., Razzari, C., Scavone, M., et al. (2015). Effect of prasugrel in patients with asthma: Results of PRINA, a randomized, double-blind, placebo-controlled, cross-over study. *Journal of Thrombosis and Haemostasis, 13*, 136–141.

Middleton, E. A., Weyrich, A. S., & Zimmerman, G. A. (2016). Platelets in pulmonary immune responses and inflammatory lung diseases. *Physiological Reviews, 96*, 1211–1259.

Nachman, R. L., & Weksler, B. (1972). The platelet as an inflammatory cell. *Annals of the New York Academy of Sciences, 201*, 131–137.

Ortiz-Muñoz, G., Mallavia, B., Bins, A., Headley, M., Krummel, M. F., & Looney, M. R. (2014). Aspirin-triggered 15-epi-lipoxin A4 regulates neutrophil-platelet aggregation and attenuates acute lung injury in mice. *Blood. 124*, 2625–2634.

Page, C. P. (1988). The involvement of platelets in non-thrombotic processes. *Trends in Pharmacological Sciences, 9*, 66–71.

Page, C. P., Paul, W., & Morley, J. (1982). An in vivo model for studying platelet aggregation and disaggregation. *Thrombosis and Haemostasis, 47*, 210–213.

Pavasini, R., Biscaglia, S., d'Ascenzo, F., Del Franco, A., Contoli, M., Zaraket, F., et al. (2016). Antiplatelet treatment reduces all-cause mortality in COPD patients: A systematic review and meta-analysis. *COPD. 13*, 509–514.

Pitchford, S. C. (2006). Novel uses for anti-platelet agents as anti-inflammatory drugs. *British Journal of Pharmacology, 152*, 987–1002.

Pitchford, S. C., Momi, S., Baglioni, S., Casali, L., Giannini, S., Rossi, R., et al. (2008). Allergen induces the migration of platelets to lung tissue in allergic asthma. *American Journal of Respiratory and Critical Care Medicine, 177*, 604–612.

Pitchford, S. C., Momi, S., Giannini, S., Casali, L., Spina, D., Page, C. P., et al. (2005). Platelet P-selectin is required for pulmonary eosinophil and lymphocyte recruitment in a murine model of allergic inflammation. *Blood. 105*, 2074–2081.

Pitchford, S. C., Riffo-Vasquez, Y., Sousa, A., Momi, S., Gresele, P., Spina, D., et al. (2004). Platelets are necessary for airway wall remodeling in a murine model of chronic allergic inflammation. *Blood. 103*, 639–647.

Pitchford, S. C., Yano, H., Lever, R., Riffo-Vasquez, Y., Ciferri, S., Rose, M. J., et al. (2003). Platelets are essential for leukocyte recruitment in allergic inflammation. *The Journal of Allergy and Clinical Immunology, 112*, 109–118.

Preibisch, S., Saalfeld, S., & Tomancak, P. (2009). Globally optimal stitching of tiled 3D microscopic image acquisitions. *Bioinformatics. 25*, 1463–1465.

Ruifrok, A. C., & Johnston, D. A. (2001). Quantification of histochemical staining by color deconvolution. *Analytical and Quantitative Cytology and Histology, 23*, 291–299.

Rylander, R., Beijer, L., Lantz, R. C., Burrell, R., & Sedivy, P. (1988). Modulation of pulmonary inflammation after endotoxin inhalation with a platelet-activating factor antagonist (48740 RP). *International Archives of Allergy and Applied Immunology, 86*, 303–307.

Semple, J. W., Italiano, J. E., & Freedman, J. (2011). Platelets and the immune continuum. *Nature Reviews. Immunology, 11*, 264–274.

Southam, D. S., Dolovich, M., O'Byrne, P. M., & Inman, M. D. (2002). Distribution of intranasal instillations in mice: effects of volume, time, body position, and anesthesia. *American Journal of Physiology. Lung Cellular and Molecular Physiology, 282*, L833–L839.

Su, X., Looney, M., Robriquet, L., Fang, X., & Matthay, M. A. (2004). Direct visual instillation as a method for efficient delivery of fluid into the distal airspaces of anesthetized mice. *Experimental Lung Research, 30*, 479–493.

Thomas, M. R., Outteridge, S. N., Ajjan, R. A., Phoenix, F., Sangha, G. K., Faulkner, R. E., et al. (2015). Platelet P2Y12 inhibitors reduce systemic inflammation and its prothrombotic effects in an experimental human model. *Arteriosclerosis, Thrombosis, and Vascular Biology, 35*, 2562–2570.

Toner, P., McAuley, D. F., & Shyamsundar, M. (2015). Aspirin as a potential treatment in sepsis or acute respiratory distress syndrome. *Critical Care, 19*, 374.

Tymvios, C., Jones, S., Moore, C., Pitchford, S. C., Page, C. P., & Emerson, M. (2008). Real-time measurement of non-lethal platelet thromboembolic responses in the anaesthetized mouse. *Thrombosis and Haemostasis, 99*, 435–440.

Weyrich, A. S., & Zimmerman, G. A. (2013). Platelets in lung biology. *Annual Review of Physiology, 75*, 569.

Zarbock, A., Singbartl, K., & Ley, K. (2006). Complete reversal of acid-induced acute lung injury by blocking of platelet-neutrophil aggregation. *The Journal of Clinical Investigation, 116*, 3211.